https://doi.org/10.48048/tis.2024.7645

An Adjusted Waveguide Antenna with A Woodpile-Shaped EBG for Eucalyptus Wood Moisture Content Measurement

Watcharaphon Naktong[1], Korn Puangnak[2], Nattapong Phanthuna[3], Sawitree Prapakarn[4], Natthapong Prapakarn[5] and Natchayathorn Wattikornsirikul[6,*]

[1]Department of Telecommunications Engineering, Faculty of Engineering and Technology, Rajamangala University of Technology Isan, Nakhon Ratchasima 30000, Thailand
[2]Department of Computer Engineering, Faculty of Engineering, Rajamangala University of Technology Phra Nakhon, Bangkok 10300, Thailand
[3]Department of Electrical Engineering, Faculty of Engineering, Rajamangala University of Technology Phra Nakhon, Bangkok 10300, Thailand
[4]Department of Agricultural Machinery Engineering, Faculty of Engineering and Technology, Rajamangala University of Technology Isan, Nakhon Ratchasima 30000, Thailand
[5]Department of Mechatronics Engineering, Faculty of Engineering and Technology, Rajamangala University of Technology Isan, Nakhon Ratchasima 30000, Thailand
[6]Department of Electronics and Telecommunications Engineering, Faculty of Engineering, Rajamangala University of Technology Phra Nakhon, Bangkok 10300, Thailand

([*]Corresponding author's e-mail: natchayathorn.w@rmutp.ac.th)

Received: 23 October 2023, Revised: 3 November 2023, Accepted: 10 November 2023, Published: 30 March 2024

Abstract

A rectangular waveguide antenna was tested for eucalyptus wood moisture content (MC) measurement before being used. To improve the moisture content measurement of the rectangular waveguide antenna, a woodpile-shaped Electromagnetic Band Gap (EBG) was installed by Transverse Electric (TE) arrangement. This antenna is responsible for receiving and transmitting signals which are converted from electrical energy into radio frequency energy transmitted through the air. In this research, we take advantage of the wave propagation of antennas in the air and use them to propagate waves through wood materials. To compare signal transmission power to determine moisture content in wood and the benefit of the EBG is that it acts like a convex lens to increase the strength of the waves so that they can penetrate the wood more efficiently. The results showed that woodpile-shaped EBG could increase the efficiency of receiving and transmitting signals, reduce working hours for farmers and reduce costs by about 90 %. When this antenna was tested and actually used, it was found that the frequency band that responded best to the moisture content value was 2.20 GHz. This antenna was built with an aluminum material of size 9×4×15 cm^3 and 2×6 units woodpile EBG on a 9.54×4 cm^2 Polyester Mylar base plate. There was a gain of 7.81 dBi from the original structure, or by 20 %. At a radius of 4 cm, the values of moisture content ranged from –9.46 to –42.19 dBm. At a radius of 6 cm, the values were –9.41 to –42.89 dBm. At a radius of 8 cm, the values ranged from –9.39 to –43.01 dBm, respectively. All 3 values were found to be efficient. The size was not less than 84 % compared to the general standard meter.

Keywords: Rectangular waveguide antenna, Eucalyptus wood, Electromagnetic bandgap, Efficiency, Transverse electric

Introduction

Nowadays, eucalyptus plants are widely planted all over the world and many researchers have extensively studied eucalyptus cultivation widely [1-6]. Eucalyptus is cheap, easy to grow and has many uses, such as being extracted as a mosquito and insect repellent, the essential oils are used to relieve nasal congestion and the bark is finely ground used to make incense. Eucalyptus wood can be used to make paper, construction materials, furniture, fence posts, animal stalls, scaffolding in construction and for charcoal [7-12]. The general wood charcoal gives 4,800 calories per gram of heat, whereas eucalyptus wood charcoal gives up to 7,400 calories per gram. In some manufacturing industries it is necessary to measure moisture before processing wood, such as for making fuel or making paper. Measuring moisture before processing can help operators save both cost and time. The humidity of the wood also affects the trading price between

farmers and buyers. Therefore, moisture measurement is necessary before wood processing. But because moisture meters available in the market are expensive and take a long time to measure, that is why the research team has designed an antenna that is suitable for measuring the moisture content of eucalyptus wood. From the above, this study was keen on burning eucalyptus tree trunks for charcoal, so it was necessary to measure the moisture content and find the maximum value of heating energy [9-12]. Before the wood is used, it must be dried in hot air or exposed to the sun before the moisture content is measured, which wastes a lot of time and money. Although some companies manufacture moisture meters using ultrasonic or voltage fluctuations for efficiency, the devices can only measure the MC from the bark surface to the middle of the trunk. This could result in the desired moisture content not being achieved. To reduce heat energy loss, the practical usage of eucalyptus requires the lowest moisture content. Based on these challenges, this study reviewed the antennas that can transmit and receive signals by electromagnetic waves through eucalyptus trunks that have been cut off [13-18] and to subsequently increase the efficiency of the receiving-transmitter power with EBG. The following literature on the structure of rectangular and cylindrical waveguide antennas used with the EBG was reviewed: Several studies have explored the structure of waveguide antennas of various shapes which employed EBG [19-29]. A conventional rectangular horn antenna was used for transmitting and receiving X-band satellite signals at the frequencies of 8 - 12 GHz. Its gain was increased with woodpile EBG in geometry of a 2-layer wire medium structure and arranged in quadratic shape. The woodpile EBG layer 1 had a radius of 2.65 λ and layer 2 had a radius 5.3 λ with a distance from the antenna (5 λ) of 15 cm. It had a gain of 24.2 dBi at the midrange frequency of 10 GHz [19]. A conventional rectangular horn antennaincorporated a asymmetric horn waveguide with hybrid metamaterial structure, for use in the secondary radar systems at 1,030, 1,090 and 1,300 MHz. with a woodpile EBG, the gain was increased to 15.43, 15.61 and 14.46 dB, respectively, accounting for 19.7, 19.8 and 24.96 % gain over the conventional rectangular waveguide antenna structure [20]. A wideband multilayer pyramidal horn antenna using substrate-integrated gap waveguide (SIGW) technology was developed in combination with a conventional rectangular horn antenna in active Ka-Band via surface aggregation gap waveguide. Metallic vias were used to surround the horn opening at each layer to control the leakage from the horn substrate designed for use at frequencies 28.5 - 35 GHz, and had a gain of 11.5 dBi at [21]. Thegain of a circular horn antennas for X-band satellite transceiver applications designed for 10 GHz frequency was increased with woodpile EBG. The antenna had a geometry of 1-layer wire structure with a quadratic shape arrangement and a distance from the antenna (16.5 λ) of 49.5 cm, with a resulting gain of 25.34 dBi [22]. A circular horn antenna for X-band satellite transceiver applications with a geometry 2-layer wire structure designed for 10 GHz had its gain enhanced with woodpile EBG. The structure was separated by a polyamide sheet, arranged in a planar shape with the end of the antenna, resulting to a a gain of 20.9 dB, which was a 15.31 % increase compared to the original antenna structure [23]. An cantenna was developed for monitoring applications of moisture content and goat manure density at 2.60 GHz, and was optimized with 1×6 woodpile EBG. It had a geometric shape with a planar shaped wire frame arranged with the end of the cantenna resulting to a gain of 9.31 dBi, an increase of 21.37 % . The results from the moisture content measurements at 1 - 100 % wb with a wave power in the range 0.0001 - 0.5 MW could measure as low as 0.14 % wb at an average power of 0.5 MW [24]. A circular horn antenna configuration hybrid antenna was developed for X-band satellite transceiver applications and was designed to operate at frequencies 10 - 14 GHz. The gain was increased with a superstrate made of 2-stacked dielectric slabs, a perfect electric conductor Fabry-Perot resonator antenna with small footprint. It was arranged in a conical waveguide with a distance of 13 mm from the antenna resulting to a gain of 19.1 dBi or 19.37 % compared to the original antenna structure [25]. A waveguide for X-band satellite transceiver applications in the frequency range of 10 - 11.5 GHz had its gain increased with a grid geometry obtained by crossing orthogonal alignments of square cross-section rods. It was configured to a planar shape with a distance of 15 mm to the end of the waveguide. It had a maximum gain of 16.2 dBi at a frequency of 11.9 GHz [26]. A waveguide with grid geometry had its gain improved by scaling square cross-section rods, at rewsulting to a maximum gain of 17.8 dBi at 10 GHz [27] and 15 dBi at 10.5 GHz [28]. A 2-port substrate-integrated waveguide (SIW) antenna with a central, double-slotted, metallic plate flanked by 2 pairs of corrugations, which was used in radar systems at frequencies of 10.15 - 11.58 GHz, had a maximum gain equal to 7 dBi [29].

Another interesting antenna structure that is being studied further is the EBG compatible microstrip antenna present in [30-34]. A microstrip antenna with multi-sources excitation for wi-fi transceivers operating at 5.8 GHz employed a mono-source EBG-antenna consisting of 3 Neltec-NY926 layers. It was planar shaped with a microstrip 4×4 array antenna with a pitch of 26.4 mm, which had a maximum gain of 6.8 dB [30]. A micro-strip antenna structure used in transmitting and receiving X-band satellite signals at a frequency of 9.5 GHz, employed a 5×5 square loop plate to enhance its gain. It had a

planar shape on the back of the microstrip with a distance of 6.5 mm from the antenna, resulting to a maximum gain of 9.5 dB. The gain value increased by 36.84 % [31]. A micromachined CPW-fed patch source and a 2-layer metamaterial superstrate for X-band satellite transceiver applications, designed for use at frequencies 8 - 12 GHz, had the gain enhanced with a 5×5 square sheet. It had a planar shape in front of the microstrip with a distance of 20 mm from the antenna, had a maximum gain of 13 dBi, which increased by 38.46 % [32]. A microstrip antenna structure operating at a frequency of 2.45 GHz was designed for energy harvesting with a rectifier circuit to convert the AC signal to DC transmissions. The gain was enhanced with a mushroom-shaped EBG that could direct the propagation, which had a 2×5 I-shaped groove placed 10 mm in front of the microstrip and 20 mm from the antenna. It had a gain of 39.76 % compared to the original antenna. The best power harvest was at an angle of 45 ° at 1 m. The gain voltage was 2.82 mV, current was 0.34 mA, and power was 0.95 uW, with gain efficiency energy of 95.88 % [33]. The rectangular antenna is used to transmit X-band signals to increase gain efficiency with a 4-layer woodpile shaped EBG type. It was arranged in the TE, TM plane and was tested at an operating frequency of 8 - 12 GHz. It was found that the gain strength increased by 18 dB [34].

The literature review highlighted waveguide antenna structures [25-28] that used woodpile EBG to increase gain [19-24]. Based on the above, this study aimed to design a waveguide antenna structure that was simple and could adjust measurement efficiency of the moisture content in eucalyptus wood as desired. In section 2, the moisture value were verified by calculation, a prototype waveguide antenna was designed for simulation, which was compared to the measurement results of the waveguide antenna with the EBG. The moisture content of eucalyptus wood was tested in section 3, a comparison of the properties of the prototype antenna structure with EBG and those of past research were done in section 4 and research was summarized and concluded in section 5.

Materials and methods

Design and measurement of waveguide antenna structural properties

Waveguide antenna structure design

In this experiment, the rectangular waveguide antenna from research [24] and [35,36] was used to determine the moisture content of eucalyptus wood with a diameter (a) = 4, 6 and 8 cm. The antenna was placed in 3 configurations: Transverse (R) = 0 °, oblique (R) = 45 ° and parallel (R) = 90 ° to the probe, as shown in **Figure 1(a)** and the antenna placement can be clearly seen in **Figure 1(b)**. The average energy value was calculated and the moisture content measurement tested and compared. The frequency ranged from 0.50 - 3 GHz and the average power (dBm) for all 4 sizes of eucalyptus trunks that were cut 24 h prior. Measurements were repeated 10 times per frequency band. It was found that the rectangular waveguide antenna was able to measure the best. The 2.20 GHz frequency band had the highest power efficiency as shown in **Figure 1(c)**. Therefore, the 2.20 GHz frequency band was calculated as Eqs. (1) - (7) [8,9,11,12] designed on aluminum sheet with a thickness of (h_1) = 0.1 cm, and the size of 9.54×4×14.60 cm^3 as in **Figure 2(a)**. When the actual antenna structure was measured, it was found that the impedance bandwidth of the operating frequency was 4.15 % (2.12 - 2.21 GHz) as in **Figure 2(b)** and the gain was 6.31 dBi. Specific direction covered the desired frequency band.

Calculation of cutoff wavelengths λ_c = 19.08 cm Eq. (1);

$$\lambda_c = \frac{2\pi}{\sqrt{\left(\frac{m\pi}{a}\right)^2+\left(\frac{n\pi}{b}\right)^2}} \quad (1)$$

Calculation of conductor wavelengths λ_g = 19.47 cm Eq. (2);

$$\lambda_g = \frac{\lambda}{\sqrt{1-\left(\frac{\lambda}{\lambda_c}\right)^2}} \quad (2)$$

Calculation of probe length L_1 = 3.40 cm Eq. (3);

$$L_1 = \frac{c}{4f_r} \quad (3)$$

Calculation of the length of the probe to the open end of a rectangular waveguide L_2 = 9.73 cm Eq. (4);

$$L_2 = \frac{\lambda g}{2} \tag{4}$$

Calculation of the length of the probe to the back end of a rectangular waveguide L_3 = 4.86 cm Eq. (5);

$$L_3 = \frac{\lambda g}{4} \tag{5}$$

Calculation of the length of the open-end of a rectangular waveguide L_4 = 14.60 cm Eq. (6);

$$L_4 = \frac{3\lambda_g}{4} \tag{6}$$

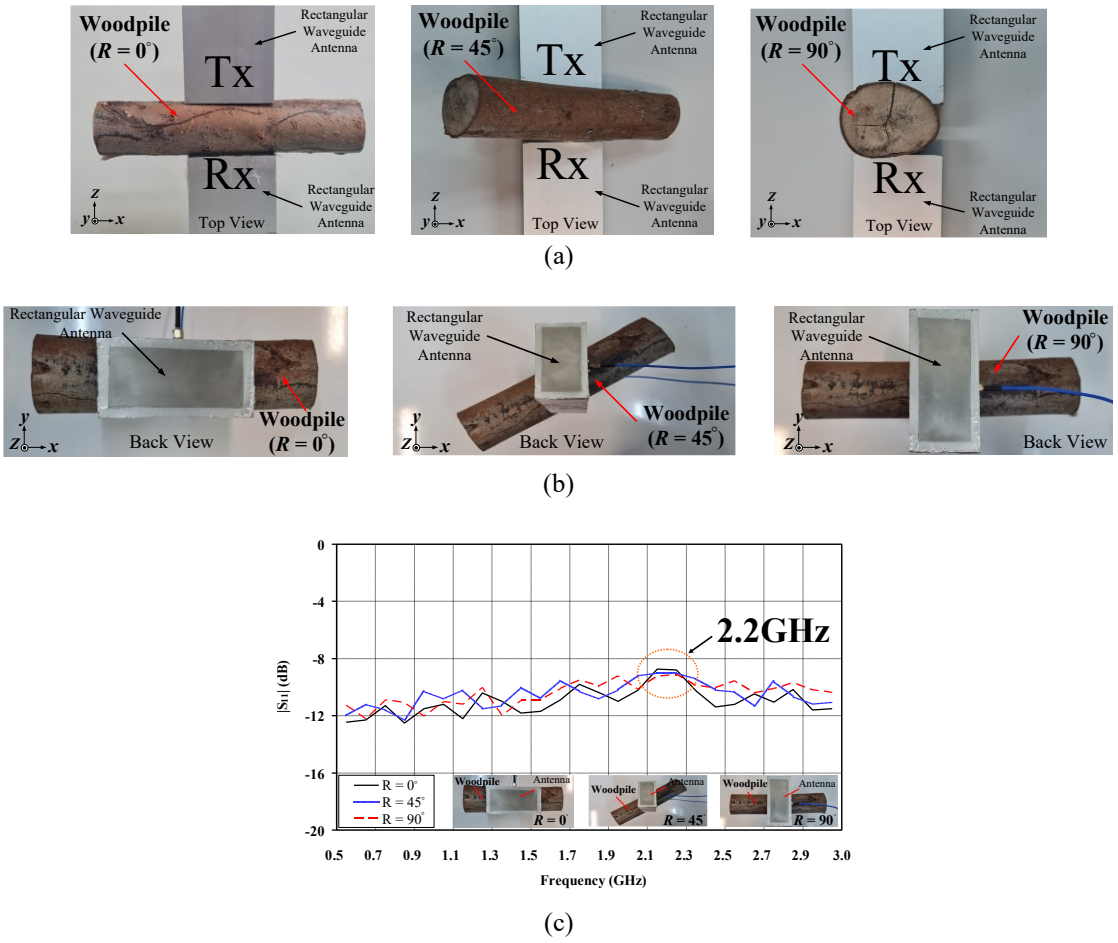

Figure 1 The moisture content of eucalyptus wood as determined by both types of waveguide antennas. (a) Rectangular waveguide antenna top view, (b) Rectangular waveguide antenna back view, and (c) $|S_{11}|(dB)$ Measurement of the moisture content at (R) = 0, 45, 90 °.

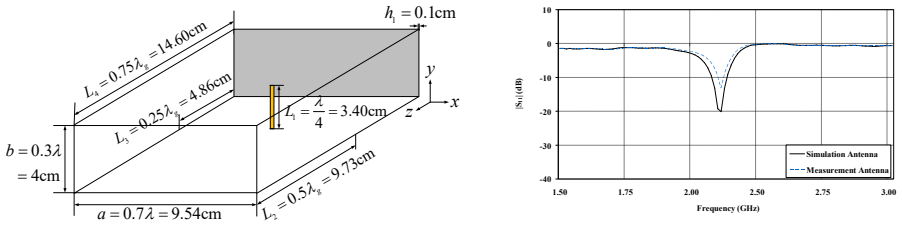

(a) (b)

Figure 2 Antenna structure design and measurement comparison simulation. (a) Rectangular waveguide antenna and (b) $|S_{11}|(\mathrm{dB})$.

Results and discussion

In the experiment, the *antenna* at 2.20 GHz was used in conjunction with woodpile EBG [22-24], as in **Figure 3(a)**, and simulated on a polyester mylar film base plate with the thickness of a base material (h_2) = 0.03 cm. The dielectric constant (ε_r) = 3.2. The thickness value of copper conductor material ($t_{1,2}$) = 0.0297 cm. The width of the EBG had a wave amplitude of 0.037 λ < W_1 < 0.098 λ.The distance (W_1) was adjusted from 0.5, 0.9 and 1.3 cm. (W_2) = 4 cm. The gap between vertical EBGs (g_1) = 0.82 cm. The inner length was set to a constant of 1.72 cm (d_1). The width of the EBG had a wavelength of 0.018 λ < W_3 < 0.056 λ. The distance (W_3) was adjusted from 0.25, 0.5 and 0.75 cm. The adjustment revealed the best value was (W_3) = 0.5 cm and the constant of the width of the vertical EBG (W_4) = 9.54 cm. The gap between each vertical EBGs (g_1) = 0.82 cm. The outer length (d_2) was adjusted from 1, 1.5, 2, 2.5 and 3 cm. The results showed that the 2.2 GHz wave entering from port 1 was directed to port 2. The cell design did not allow for a 2.20 GHz response which changed the loop dimension, impacting the transmission coefficient. The curve was moved to another frequency with the best effect where the inner length (d_1) was 1.72 cm outer length (d_2) was 2 cm as shown in **Figure 3(b)**. This had a positive effect on gain including the wave propagation in front of the eucalyptus surface. According to the graph, the electrical permittivity of the proposed line medium structure was close to 0, and for frequencies less than 0.8 GHz, the electrical permittivity was negative. This was a property of the metamaterial as shown in **Figure 3(b)**, which could allow waves to propagate at the 2.20 GHz band. It had an increased gain of 8.16 dBi compared to the Strip line medium, which can be calculated from Eqs. (7) - (10) [23-24]. The width between EBG ($d_{1,2}$) can be calculated from Eqs. (11) - (12) [26-28].

$$k_p^2 = \frac{2\pi}{(W_1)^2\left[\ln(W_1/2\pi t_1)+0.5275\right]} \tag{7}$$

$$\varepsilon_{SM} = \varepsilon_0\varepsilon_{rh}\left(1-\frac{k_p^2}{\varepsilon_{rh}k_0^2-k_y^2}\right) \quad :k_0^2 = \left(\frac{\omega}{c\varepsilon_h}\right)^2 \tag{8}$$

$$d_1 = \frac{W_1}{0.523} \tag{9}$$

where k_p = plasma frequency

ε_{SM} = Effective permittivity strip line medium

d_1 = The width of the horizontal EBG base

d_2 = The width of the vertical EBG base

The simulation results were used in a new configuration to find the best gain, Transverse Electric (TE) polarization and Transverse Magnetic (TM) polarization as shown in **Figure 3** Woodpile arrangement of 2×6 units was adjusted at distance (h_3) from 0.1 to 6 cm, as shown in **Figure 4** which was simulated through the Computer Simulation Technology (CST) program. The structure had a gain of 8.16 dBi at distance (h_3) of 0.1 cm, which was an increase from 6.31 dBi as shown in **Figure 5** Which is obtained by simulating the c program CST 0.1 - 6 cm [34] as the results are shown in **Table 1** at a working frequency range of 2 - 3.5 GHz as in **Figure 6**. Various parameters from the best adjustment are shown in **Table 3**.

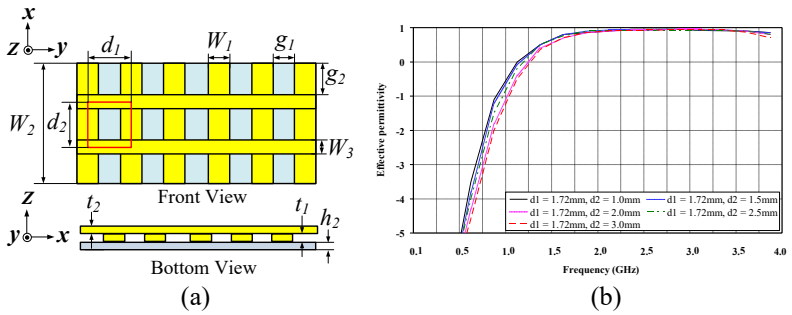

Figure 3 Simulation of the EBG structure. (a) Unit cell of I-shaped and (b) Effective permittivity.

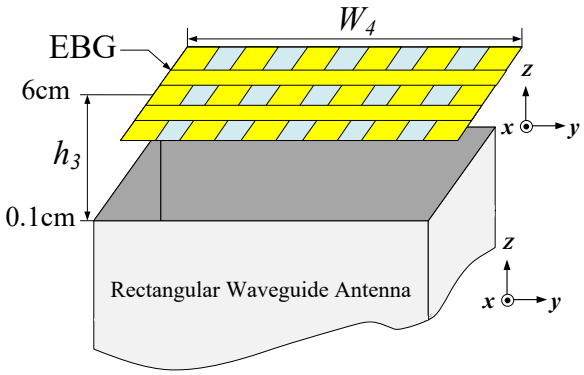

Figure 4 Simulation distance between rectangular waveguide antenna and EBG.

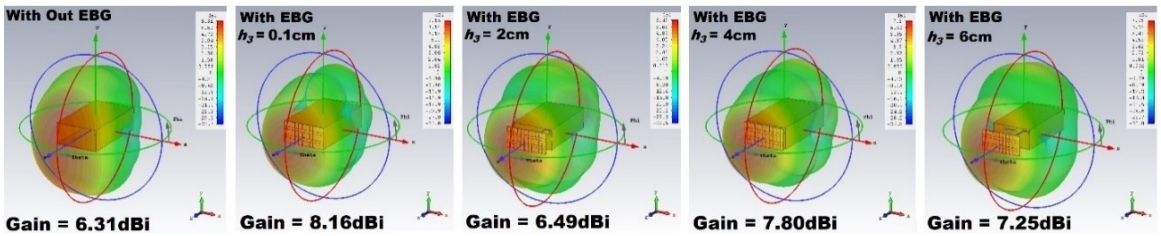

Figure 5 3D radiation pattern of an antenna in conjunction with EBG.

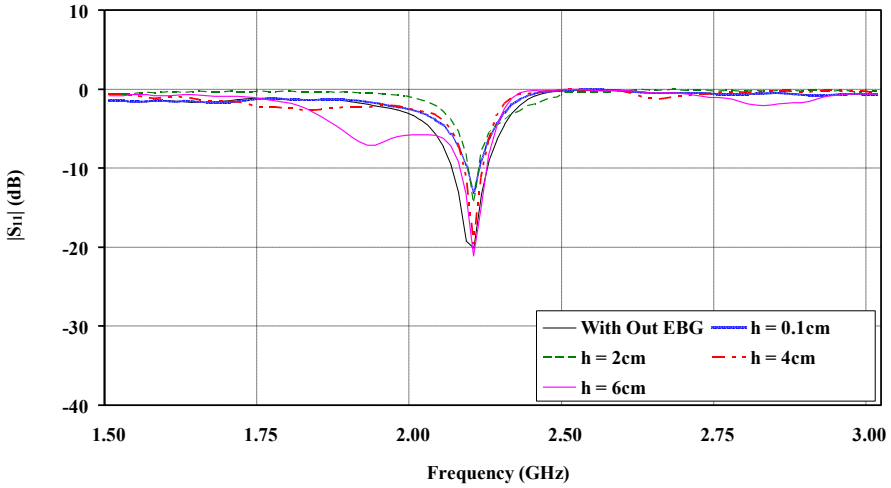

Figure 6 Simulation of value $|S_{11}|(dB)$ from adjusting the h_3.

Table 1 Distance between rectangular waveguide antenna combined with the EBG, at the frequency of 2.20 GHz.

Distance between rectangular waveguide antenna and EBG (cm)	Gain (dBi)
0.1	8.16
2	6.49
4	7.80
6	7.25

Table 2 Comparison of measuring properties of rectangular waveguide antennas combined with EBG, at the frequency of 2.20 GHz.

Antenna	$\lvert S_{11}\rvert(\mathrm{dB})$	VSWR	Gain (dBi)	Z_{in} (Ω)
Waveguide antenna without EBG	–20.01	1.09:1	6.31	47.53 + j6.63
Waveguide antenna with EBG, a distance of 0.1 cm	–12.52	1.43:1	8.16	41.99 + j52.32

Table 3 Size parameters of rectangular waveguide antennas with EBG.

Variable	Meaning	Size (cm)
a	The width of rectangular waveguide antenna	9.54
b	The length of rectangular waveguide	4
L_1	The length of monopole antenna	3.40
L_2	The distance from monopole antenna to the front end of rectangular waveguide.	9.73
L_3	The distance from monopole antenna to the back end of rectangular waveguide	4.86
L_4	The length of the rectangular waveguide tube	14.60
W_1	The width of the horizontal EBG	0.9
W_2	The width of the vertical EBG	4
W_3	The width of the horizontal EBG base	0.5
W_4	The width of the vertical EBG base	9.54
h_1	The thickness of rectangular waveguide	0.1
h_2	The length of polyester mylar film base plate	0.03
h_3	The distance between EBG and the open end of rectangular waveguide	6
d_1	The width of the horizontal EBG base	1.72
d_2	The width of the vertical EBG base	2
t_1	The thickness of copper conductor material of EBG in TE polarization arrangement	0.0297
t_2	The thickness of copper conductor material of EBG in TM polarization arrangement	0.0297
g_1	The distance between each EBGs in TE polarization arrangement	0.82
g_2	The distance between each EBGs in TM polarization	1

Measurement of antenna properties

The rectangular waveguide antenna with woodpile EBG antenna properties was measured by Network Analyzer model E5071C as shown in **Figure 7**. It was found that the operating frequency range was 17.14 % (1.92 - 2.28 GHz) as in **Figure 8**, the impedance Z_{in} = 44 + j63.31 Ω and a gain was 7.81 dBi, which was displayed in **Table 4**. The energy propagation was directional in both measurement and simulation. It also has the advantage of being able to radiate energy through wood better and with higher accuracy than the prototype waveguide antennas without EBG, which will show the power measurement results in the next section results as shown in **Figure 9**.

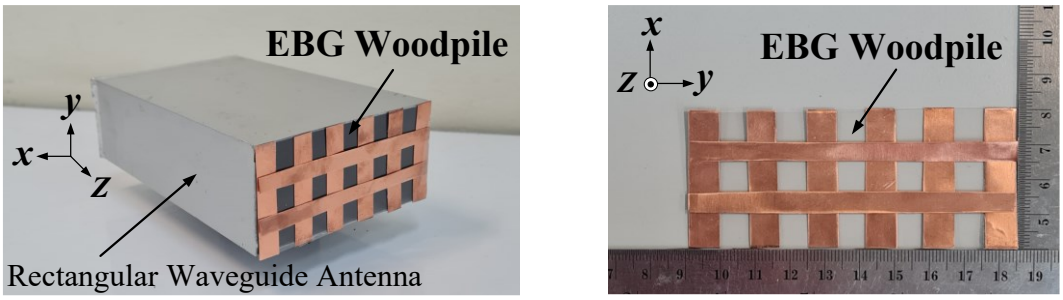

(a) (b)

Figure 7 Rectangular waveguide antenna with woodpile EBG. (a) The rectangular waveguide antenna and (b) Woodpile EGG with Woodpile EBG.

Table 4 Comparison of measurement properties of rectangular waveguide antenna with EBG at 2.20 GHz.

	k	$\|S_{11}\|$(dB)	VSWR	Gain (dBi)	Z_{in} (Ω)
Simulation	Waveguide antenna	–20.01	1.09:1	6.31	47.53 + j6.63
	Waveguide antenna with EBG	–12.52	1.43:1	8.16	41.99 + j52.32
Measurement	Waveguide antenna	–17.68	1.24:1	5.97	53 + j39.17
	Waveguide antenna with EBG	–14.95	1.38:1	7.81	44 + j63.31

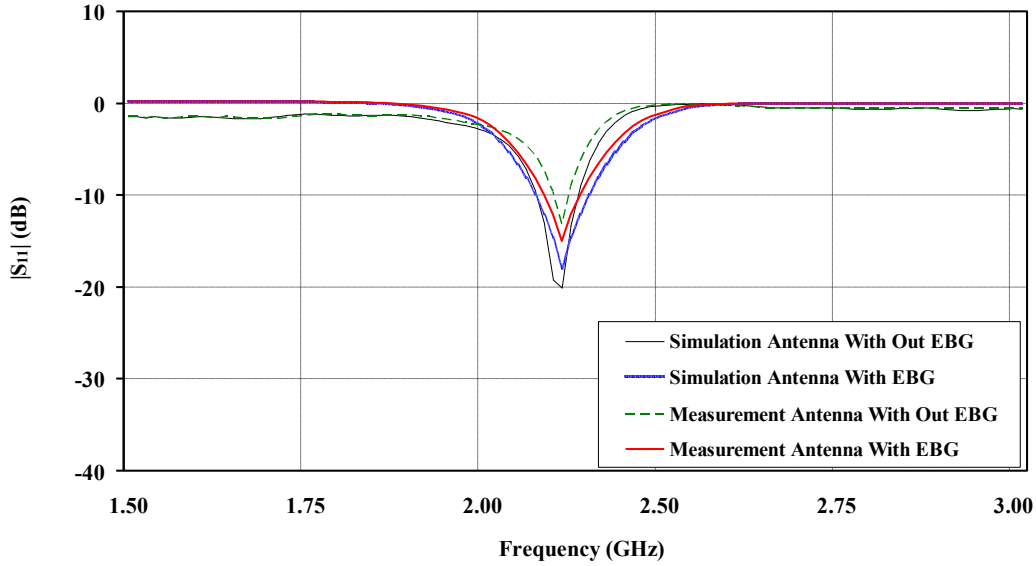

Figure 8 Comparison of simulation results and measurement results $|S_{11}|$(dB).

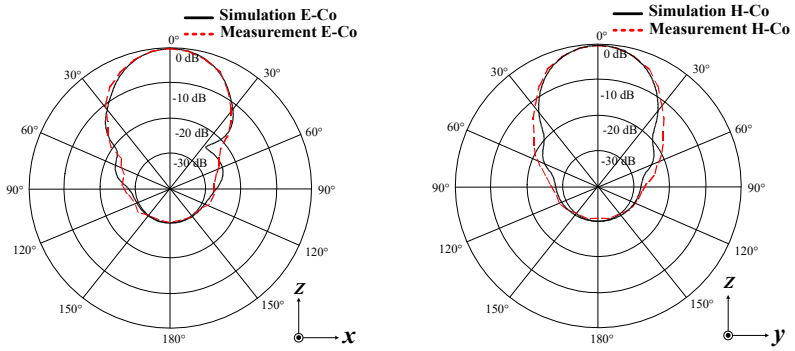

(a) (b)

Figure 9 Comparison of electric and magnetic field radiation energy forms of the simulation and the measurement results. (a) Electric field and (b) Magnetic field.

Frequency testing to measure moisture content of eucalyptus wood

The measurement test procedure involves using the designed antenna and EBG to act as receiver and transmitter on both sides. As for the transmitter, the antenna will be connected to the Nano Lite VNA 2.2 transmitter, used as a transmitter at a frequency of 2.2 GHz, strength at 0 dBm. Then the signal will be sent through the eucalyptus wood to the receiver to convert the wave strength energy into alternating current using a voltage doubler circuit. The voltage value is sent to the Arduino Nano board to display the voltage value on the LCD Display. Tests were done on 4 sizes of eucalyptus trunks that were cut 1 - 3 days prior, to reduce the moisture content of the wood to the desired level at the range of 1 - 100 % wb. as desired. The measurement was repeated 10 times. Measurements were done with a Lite VNA transmitter model 64, which was set to 0 dBm or 1 MW signal strength as shown in **Figure 10** [37]. The efficiency in measuring humidity of the antenna for measuring 3 sizes of wood using a strength of 0.1 MW. It was found that it can actually measure through the wood. Then the measured values were compared with the moisture wood, It was found that if the moisture was high, the strength of the antenna signal decreased. On the other hand, if the moisture in the wood is low, the signal strength will increase accordingly. Factors affecting the variation in frequency used in moisture analysis depend on the size, texture and density of the wood. The resonance measurements were performed with a prototype rectangular waveguide antenna with a prototype rectangular waveguide antenna with woodpile EBG that transmits frequency energy through the wood to the receiver with greater efficiency than the original antenna. By measuring on the eucalyptus logs with diameter of(a) = 4, 6 and 8 cm. The length of eucalyptus log (H) = 26 cm. The moisture content was measured at the width of the eucalyptus trunk, in 3 points: The top was, the middle and the bottom. Ten pieces of each size were selected for the tests. The measurements were performed to find the best energy for assessing moisture content of the wood measured at the range of 1 - 100 % wb. The test showed that at a radius of 4 cm the energy ranged from –9.46 to –42.19 dBm, –9.41 to –42.89 dBm at a radius of 6 cm and –9.39 to –43.01 dBm at a radius of 8 cm, as shown in **Figure 11**. The energy values at all 3 points of the eucalyptus trunks were found to be comparable; however, the moisture content of the different radii differed, ranging from 3 - 57 % wb. The size of the different widths of eucalyptus trees significantly affected the transmittance, as shown in **Figure 11**, which was used to calculate the moisture content. The moisture content was calculated as in Eq. (12) [38]. The highest heating value was 18,550 kJ/kg as shown in **Figure 12** [39]. The energy value comparison showed an average of about –9.40 to –43 dBm, indicating the moisture content value compared to the energy value as seen in **Table 5**.

Calculation of moisture content (MC) as Eq. (12);

$$\text{MC}\ (\%) = \frac{\text{SWBB-SWAB}}{\text{SWBB}} \times 100 \tag{12}$$

where MC = Moisture Content (%wb)
SWBB = Sample Weight Before Baking (g)
SWAB = Sample Weight After Baking (g)

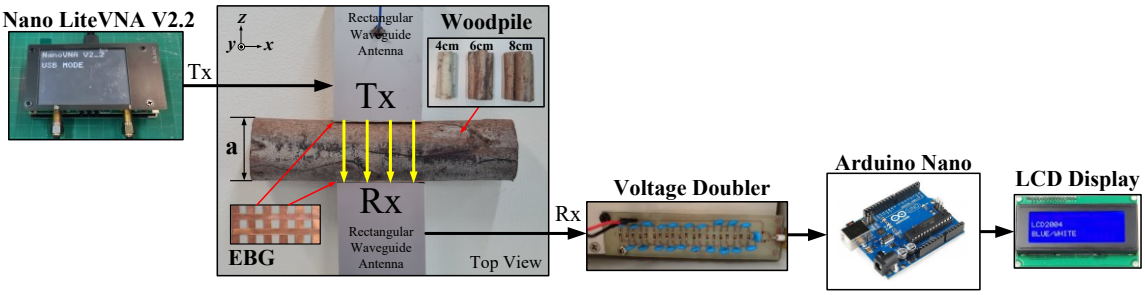

Figure 10 Eucalyptus wood moisture content measurement test using a rectangular waveguide antenna.

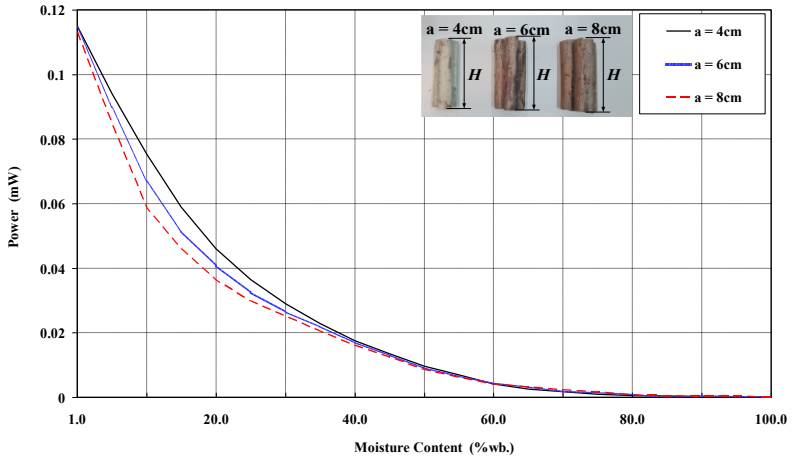

Figure 11 Moisture content measurement results of eucalyptus wood at diameters of 4, 6 and 8 cm.

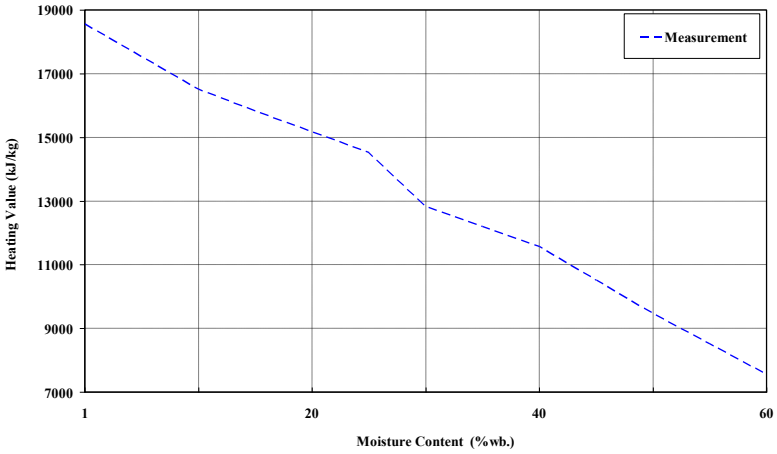

Figure 12 Heating value measurement results.

Table 5 Measure the moisture content of all 3 sizes of wood.

Radius value of wood (cm)	Receiving energy at 0 - 100 % moisture content (dBm)	(MW)	Moisture content 0 - 100 % compared to heating value (kJ/kg)	Distance (cm)	Efficiency (%)
4	–9.40 to –42.19	0.11 to 0.000060		4	87.01
6	–9.41 to –42.89	0.11 to 0.000051	18,550 to 7,550	6	85.68
8	–9.39 to –43.01	0.11 to 0.000050		8	84.57

To test the hypothesis that the thickness of the eucalyptus wood and the percentage of moisture in the wood affect the energy in MW. Reference statistical analysis It is an analysis of the difference between the percentage of moisture in the wood with the size and thickness of the eucalyptus wood in the cm unite. This can be done by using the 2-way ANOVA analysis technique to analyze the relationship between the percentage of moisture in the wood with the size and thickness of the eucalyptus wood, whether it affects the energy in MW or not. And analyze the relationship between wood thickness and moisture percentage using multiple regression analysis to test the hypothesis that the thickness of the eucalyptus wood and the percentage of moisture in the wood affect the energy in MW.

Table 6 Analysis of the percentage of wood moisture and the thickness of the wood affecting energy in MW (2-way ANOWA).

Factor determinants the percentage of wood moisture and the thickness of eucalyptus wood	**Test statistics value**	***p*-value**
Percentage of eucalyptus wood moisture	F-statistics = 84.32	0.000*
Thickness of eucalyptus wood	F-statistics = 0.65	0.523
The amount of data 299, R squared 74.36 %is statistically significant at the 0. 05level.		

The amount of data 299, R squared 74.36 % is statistically significant at the 0.05 level.

Table 6 found that the percentage of wood moisture factors affecting the energy value in MW were significantly, different at the 0.05 level. As for the factor of thickness of eucalyptus wood affecting the energy value in MW, the value was not significantly different at the 0.05 level.

Testing the hypothesis that the thickness of eucalyptus wood and the percentage of moisture in the wood affect energy in MW.

Table 7 shows the statistical values of the multiple regression analysis of the variable percentage of wood moisture and the thickness of eucalyptus wood.

Factor determinants the percentage of wood moisture and the thickness of eucalyptus wood	**Coefficient**	**Std.Error**	***p*-value**
Constant	0.055559	0.004141	0.000
Percentage of eucalyptus wood moisture	–0.00065747	0.00003383	0.000*
Thickness of eucalyptus wood	–0.0002681	0.0005950	0.653

The amount of data 299, R Squared 56.0 % is statistically significant at the 0.05 level.
The regression equation is y = 0.0556–0.000657×–0.000268T.

From **Table 7**, when considered overall, it was found that the independent variable of eucalyptus wood moisture percentage affected the MW energy value with statistical significance at the 0.05 level. The R square value is 56 %, that is, all variables can explain 56 % of the change of energy in MW unite of the test measurement.

Comparison of research

The comparative study as shown in **Table 8** revealed that the proposed antenna structure with EBG had an advantage of being less complex than the studies [19-23] and [25-29], except for the studies [24]. The distance between the proposed antenna and the EBG was less than the studies [24-28], which was 0.1 mm. In addition, the proposed antenna was thin, lightweight EBG, had a simple design and had a flexibility according to the structure of eucalyptus wood. The gain was less than that of structural antennas in the studies [19-29], due to the distance between the antenna and the EBG and the high frequency range which affected the gain, making it higher.

Table 8 Comparison efficiency of rectenna.

Reference	Frequency (GHz)	Antenna shape and EBG shape		Arrangement	EBG size (cm^3)	Distance EBG (cm)	Gain (dBi)
		Antenna shape	EBG shape				
[19]	8 - 12	Conical Horn	Wire Wire	TE	7.95×1.5 15.9×1.5	15 -	24.20
[20]	1.09, 1.30	Asymmetric Horn	Woodpile	TE, TM	31.81×31.81×7.62	4	15.61 14.46
[21]	28.5 - 35	Horn	Wire	TE	3×1.9×0.6	-	11.50
[22]	10	Conical Horn	Woodpile	TE	15.12×0.16	49.50	25.34
[23]	10	Conical Horn	Woodpile	TE	6×6×0.6	-	20.90
[24]	2.56 - 2.65	Cantenna	Woodpile	TE	6×6×0.0597	3	9.31
[25]	10 - 15	Rectangular Waveguide	Rectangular	TE	3.4×3.4×0.48	13	15.40
[26]	11.90	Rectangular Waveguide	Square cross-Section rods	TE, TM	4.5×4.5×1	1.50	16.20
]27]	11.90	Rectangular Waveguide	Square cross-Section rods	TE, TM	6×6×1.6	1.50	16.10
]28]	11.90	Rectangular Waveguide	Square cross-Section rods	TE, TM	4.5×4.5×1	1.50	12.50
[29]	10.15 - 11.58	monopole antenna	I-shaped	TE	6.3×5.4×0.6	-	7
Proposed	1.91 - 2.33	Rectangular Waveguide	Woodpile	TE, TM	9.54×4×0.09	0.10	7.81

Conclusions

A rectangular waveguide antenna that was designed at a 2.20 GHz frequency band and used in with the EBG of 2×6 units yielded the best moisture measurement in eucalyptus wood. The advantage of this research is that it reduces the time to measure humidity, which is faster than a dehumidifying moisture meter. Dehumidifying moisture meters require 6 - 12 h of work time, depending on the humidity value and the quality of the meter. And another advantage of the measuring device from this research is that it is cheap. But there are still disadvantages in other variables namely the size of the wood, the smoothness of the surface, and the density of the wood. The antenna was tested on eucalyptus tree trunks with diameters (a)= 4, 6 and 8 cm. The measurement of the moisture content ranging from 1 - 100 % wb showed a power value average of about –9 to –43 dBm or 0.11 to 0.00006 MW. The highest heating value was 18,550 to 7,550 kJ/kg, which had efficiency values of 87.01, 85.68 and 84.57 %. Because the signal transmission distance varied depending on the size of the eucalyptus tree trunk and the structure of the eucalyptus tree whose surfaces were dissimilar. The proposed antenna had advantages in terms of simple construction with EBG of 2×6 units plane alignment at the end of an antenna. The gain was enhanced by 7.81 dBi, and had up to 23.55 % diffusion coverage on the surface of the eucalyptus tree plane. The results of this research can be used to measure moisture content with other types of woods in the future and has another advantage. It can help researchers measure moisture without needing to spend 6 - 12 h. Industrial factory operators can analyze moisture values before using them to produce charcoal, reducing electricity costs and time. Moreover, it will also help the community to apply it to determine the hardness of wood using this transition method and can apply knowledge to other forms of materials. The research team has studied from research on new antenna and EBG structure techniques. It helps respond to frequency adjusting as desired, including increasing the gain rate even more. To be able to find appropriate values for differences in wave transmission through other types of materials as desired from research [40-47].

Acknowledgments

We would like to thank the Department of Electronic and Telecommunications Engineering at the Faculty of Engineering, Rajamangala University of Technology Phra Nakhon, Thailand, and the Department of Telecommunications Engineering at the Faculty of Engineering and Technology, Rajamangala University of Technology Isan, Thailand, for their support in completing this research.

References

[1] U Sirijaroonwong, S Kiratiprayoon, S Diloksumpun and P Ruenrit. Some morphological characteristics of eucalyptus camaldulensis Dehn. clone A5 and clone D1, at the clonal plantation in Eastern Thailand. *Sci. Tech. Asia* 2017; **22**, 23-34.

[2] H Jessadarom, W Phetruang, S Haitook and R Cheewangkoon. Isolation of Calonectria sulawesiensis from soil in Thailand and its pathogenicity against eucalyptus camaldulensis. *Plant Pathol. Quarantine* 2018; **8**, 1-8.

[3] H Aiso-Sanada, F Ishiguri, S Diloksumpun, I Nezu, J Tanabe, J Ohshima and S Yokota. Effects of thinning on anatomical characteristics and wood properties of 12-year-old Eucalyptus camaldulensis trees planted in Thailand. *Tropics* 2019; **28**, 67-73.

[4] I Nezu, F Ishiguri, H Aiso, S Diloksumpun, J Ohshima, K Iizuka and S Yokota. Repeatability of growth characteristics and wood properties for solid wood production from *Eucalyptus camaldulensis* half-sib families growing in Thailand. *Silvae Genetica* 2020; **69**, 36-43.

[5] W Wongchai, A Promwungkwa and W Insuan. Above-ground biomass allometric equation and dynamics accumulation of eucalyptus camaldulensis and acacia hybrid plantations in Northern Thailand. *Int. J. Renew. Energ. Res.* 2020; **10**, 1664-73.

[6] C Klinsukon, S Lumyong, TW Kuyper and S Boonlue. Colonization by arbuscular mycorrhizal fungi improves salinity tolerance of eucalyptus (Eucalyptus camaldulensis) seedlings. *Sci. Rep.* 2021; **11**, 4362.

[7] H Yspeert. 2018, The design of a eucalyptus furniture manufacturing facility in Hogsback, Eastern Cape. Master Thesis. Nelson Mandela University, Port Elizabeth, South Africa.

[8] MA Sarker, MNA Mridha, MA Khaleque and MA Rahman. Machining properties of Eucalyptus (*Eucalyptus camaldulensis*) wood and its utilization potential for furniture manufacturing. *Eur. J. Eng. Tech. Res.* 2022; **7**, 63-6.

[9] DM Neiva, S Araujo, J Gominho, ADC Carneiro and H Pereira. Potential of *Eucalyptus globulus* industrial bark as a biorefinery feedstock: Chemical and fuel characterization. *Ind. Crop. Prod.* 2018; **123**, 262-70.

[10] L Volkova and CJ Weston. Effect of thinning and burning fuel reduction treatments on forest carbon and bushfire fuel hazard in Eucalyptus sieberi forests of South-Eastern Australia. *Sci. Total Environ.* 2019; **694**, 133708.

[11] B Samal, KR Vanapalli, BK Dubey, J Bhattacharya, S Chandra and I Medha. Influence of process parameters on thermal characteristics of char from co-pyrolysis of eucalyptus biomass and polystyrene: Its prospects as a solid fuel. *Energy* 2021; **232**, 121050.

[12] H Wang, PJV Eyk, PR Medwell, CK Birzer, ZF Tian, M Possell and X Huang. Smouldering fire and emission characteristics of Eucalyptus litter fuel. *Fire Mater.* 2022; **46**, 576-86.

[13] B Gal and D Nowak. Nondestructive, microwave testing of compression strength and moisture content of green molding sands. *J. Nondestr. Eval.* 2021; **40**, 86.

[14] S Taheri, G Brodie and D Gupta. Optimised ANN and SVR models for online prediction of moisture content and temperature of lentil seeds in a microwave fluidised bed dryer. *Comput. Electron. Agr.* 2021; **182**, 106003.

[15] HS Kol and B Çayır. Increasing the impregnability of oriental spruce wood via microwave pretreatment. *BioResources* 2021; **16**, 2513-23.

[16] M Radwan, DV Thiel and HG Espinosa. Single-sided microwave near-field scanning of pine wood lumber for defect detection. *Forests* 2021, **12**, 1486.

[17] C Li, C Zhao, Y Ren, X He, X Yu and Q Song. Microwave traveling-standing wave method for density-independent detection of grain moisture content. *Measurement* 2022; **198**, 111373.

[18] D Wang, X Li, X Hao, J Lv and X Chen. The effects of moisture and temperature on the microwave absorption power of poplar wood. *Forests* 2022; **13**, 309.

[19] S Kampeephat, P Kamphikul and R Wongsan. Gain improvement for conventional rectangular horn antenna with additional two-layer wire medium structure. *In*: Proceedings of the 2017 Progress in Electromagnetics Research Symposium-Fall (PIERS-FALL), Singapore. 2017, p. 2493-7.

[20] R Wongsan and P Khamsalee. Hybrid metamaterial structure for asymmetric horn of secondary radar system. *In*: Proceedings of the 2019 7th International Electrical Engineering Congress (iEECON), Hua Hin, Thailand. 2019.

[21] SM Sifat, SI Shams and AA Kishk. Ka-band integrated multilayer pyramidal horn antenna excited by substrate-integrated gap waveguide. *IEEE Trans. Antenn. Propag.* 2021; **70**, 4842-7.

[22] R Wongsan, P Krachodnok, S Kampeephat and P Kamphikul. Gain enhancement for conventional circular horn antenna by using EBG technique. *In*: Proceedings of the 2015 12th International Conference on Electrical Engineering/Electronics, Computer, Telecommunications and Information Technology (ECTI-CON), Hua Hin, Thailand. 2015.
[23] P Duangtang, P Mesawad and R Wongsan. Creating a gain enhancement technique for a conical horn antenna by adding a wire medium structure at the aperture. *J. Electromagn. Eng. Sci.* 2016, **16**, 134-42.
[24] W Naktong, S Prapakarn, N Prapakarn and N Wattikornsirikul. Cantenna adjustment with 1×6 woodpile shaped EBG for application in goat manure moisture content and bulk density monitoring. *Progr. Electromagnetics Res. C* 2022; **126**, 49-62.
[25] Y Ge, Z Sun, Z Chen and YY Chen. A high-gain wideband low-profile Fabry-Pérot resonator antenna with a conical short horn. *IEEE Antenn. Wireless Propag. Lett.* 2016; **15**, 1889-92.
[26] C Ponti, P Baccarelli, S Ceccuzzi, L Tognolatti and G Schettini. Resonant-cavity antennas with tapered and wideband EBG superstrates. *In*: Proceedings of the 2021 International Conference on Electromagnetics in Advanced Applications (ICEAA), Honolulu. 2021, p. 301-4.
[27] C Ponti, P Baccarelli, S Ceccuzzi and G Schettini. Tapered all-dielectric EBGs with 3-D additive manufacturing for high-gain resonant-cavity antennas. *IEEE Trans. Antenn. Propag.* 2020; **69**, 2473-80.
[28] C Ponti, P Baccarelli, S Ceccuzzi and G Schettini. 3D additive manufacturing of tapered EBG layers for a resonant-cavity antenna. *In*: Proceedings of the 2022 IEEE 21st Mediterranean Electrotechnical Conference (MELECON), Palermo, Italy. 2022, p. 564-8.
[29] Y Jin, H Lee and J Choi. A compact, wideband, two-port substrate-integrated waveguide antenna with a central, double-slotted, metallic plate flanked by two paired of corrugations for radar applications. *IEEE Trans. Antenn. Propag.* 2018; **66**, 6376-81.
[30] A Kaabal, ME Halaoui, BE Jaafari, S Ahyoud and A Asselman. Design of EBG antenna with multi-sources excitation for high directivity applications. *Procedia Manuf.* 2018; **22**, 598-604.
[31] S Rai and D Rao. Design of enhanced gain micro-strip antenna using square loop shaped meta-material substrate. *Int. Res. J. Eng. Tech.* 2018; **5**, 3604-9.
[32] K Kanjanasit and C Wang. A wideband resonant cavity antenna assembled using a micromachined CPW-fed patch source and a two-layer metamaterial superstrate. *IEEE Trans. Compon. Packag. Manuf.* 2018; **9**, 1142-50.
[33] W Naktong, A Ruengwaree, N Fhafhiem and P Krachodnok. Resonator rectenna design based on metamaterials for low-RF energy harvesting. *Comput. Mater. Continua* 2021; **68**, 1731-50.
[34] F Frezza, L Pajewski, E Piuzzi, C Ponti and G Schettini. Radiation-enhancement properties of an X-band woodpile EBG and its application to a planar antenna. *Int. J. Antenn. Propag.* 2014; **2014**, 729187.
[35] CA Balanis. *Antenna theory analysis and design handbook*. 3rd ed. John Willey & Sons Inc., New Jersey, 1997.
[36] Y Huang. *Antennas: From theory to practice*. 2nd ed. John Wiley & Sons, New Jersey, 2021.
[37] W Naktong, S Phonsri, P Boonmaitree, P Thitimahatthanagusul, A Innok, S Kornsing, S Prapakarn, S Sakulchat, T Yodroj, D Kummuangmai and N Prapakarn. Measurement of moisture in wood by microwave. *In*: Proceedings of the 14th Engineering, Science, Technology and architecture Conference, Kalasin, Thailand. 2023.
[38] W Horwitz and GW Latimer. *Official methods of analysis of AOAC international*. 18th ed, AOAC International, Maryland, 2005.
[39] American Society for Testing and Materials. *Standard test method for gross calorific value of coal and coke by the adiabatic bomb calorimeter*. American Society for Testing and Materials, Pennsylvania, 1996.
[40] V Pugatch, M Borysova, A Mykhailenko, O Fedorovitch, Y Pylypchenko, V Perevertaylo, H Franz, K Wittenburg, M Schmelling and C Bauer. Micro-strip metal detector for the beam profile monitoring. *Nucl. Instrum. Meth. Phys. Res. A Accel. Spectrometers Detectors Assoc. Equip.* 2007; **581**, 531-4.
[41] D Aloisio and N Donato. Development of gas sensors on microstrip disk resonators. *Procedia Eng.* 2014; **87**, 1083-6.
[42] W Naktong and N Wattikornsirikul. Dipole antenna with horn waveguide for energy harvesting in DTV systems. *Progr. Electromagnetics Res. M* 2022; **111**, 145-57.

[43] W Naktong and N Wattikornsirikul. Dipole Antenna with 18×5 square electromagnetic band gap for applications used in monitoring children trapped in cars. *Progr. Electromagnetics Res. M* 2022; **112**, 163-76.
[44] Z Liu, Y Wang, M Li and Q Guo. Temperature self-compensation method for crack length measurement based on a microstrip antenna sensor. *IEEE Sensor. J.* 2022; **22**, 16036-45.
[45] S Promput, W Naktong, S Sakulchat and A Ruengwaree. Waveguide antenna with an inverted 3-tiered cake-shaped probe for NB-IoT applications. *In*: Proceedings of the 2023 International Electrical Engineering Congress (iEECON), Krabi, Thailand. 2023, p. 323-6.
[46] S Harikirubha, V Baranidharan, S Saranya, K Keerthana and M Nandhini. Different shapes of microstrip line design using FR4 substrate materials-A comprehensive review. *Mater. Today Proc.* 2021; **45**, 3404-8.
[47] P Santhya, V Baranidharan, JR Roy, P Yuvaraj and KT Tharun. Performance of defected ground structure with miniaturized microstrip patch antenna using RMPA substrate material. *Mater. Today Proc.* 2021; **45**, 3286-9.